Arrhythmogenic Ablation Lesions Underlie Atrial Fibrillation Recurrence: A Longitudinal Digital Twin Study

Carolyna Yamamoto[1], Syed Ali[1], Kensuke Sakata[2], Shane Loeffler[2], Adityo Prakosa[2], Eugene Kholmovski[1,2], Natalia Trayanova[1,2]

[1] Johns Hopkins University, Baltimore, United States
[2] Alliance for Cardiovascular Diagnostic and Treatment Innovation, Baltimore, United States

Abstract

Atrial fibrillation (AF) recurrence following catheter ablation remains a significant clinical challenge. This study investigates whether recurrence could result from the incomplete elimination of the native arrhythmogenic substrate or from new pro-arrhythmic substrates created by ablation. Patient-specific computational models of the atria (i.e., digital twins; DTs) constructed from pre- and post-ablation delayed-enhancement magnetic resonance imaging (MRI) scans were used to assess the arrhythmogenic substrate before and after the procedure. Our findings reveal that the ablation procedure had a differential effect on the substrate of patients whose AF did and did not recur, and suggest that recurrence may be facilitated by ablation lesions themselves. This work presents a novel framework using longitudinal bi-atrial DTs and demonstrates the value of computational models in elucidating the mechanisms underlying AF recurrence.

1. Introduction

Atrial fibrillation is characterized by disorganized electrical activity in the atria, leading to ineffective atrial contraction and loss of the normal rhythm of the heart. Catheter ablation is a key treatment for AF aimed at disrupting abnormal electrical activity to restore normal rhythm. However, many patients experience recurrence [1], highlighting a significant clinical challenge in achieving long-term rhythm control.

The mechanisms underlying AF are complex and multifactorial, involving a combination of ectopic triggers, structural remodeling, and other factors. Fibrotic remodeling leads to regions of slow conduction that could harbor reentrant circuits [2], creating an arrhythmogenic substrate for AF. Ablation lesions lead to further remodeling (scarring) of the atrial myocardium, which may inadvertently create new arrhythmogenic substrates. The relationship between ablation-induced scars and AF recurrence is complex and not fully understood.

Due to the limited ability to assess patient-specific electrophysiological (EP) effects of structural remodeling in vivo, computational heart models offer a valuable tool for mechanistic studies of cardiac arrhythmias [2, 3]. In this study, we employed bi-atrial computational models to investigate whether AF recurrence could be due to the incomplete elimination of the native arrhythmogenic substrate or the creation of new pro-arrhythmic regions by the ablation lesions. We constructed bi-atrial DTs from pre- and post-ablation MRI scans of AF patients and evaluated the arrhythmogenic propensity of the atrial substrate before and after the procedure. Our results shed new light on the role of ablation scarring in substrate arrhythmogenesis and AF recurrence.

2. Methods

2.1. Clinical Data

Patients with symptomatic AF undergoing first-time catheter ablation as part of routine care underwent cardiac MRI before and three months after ablation. The ablation procedure was conducted following established techniques for pulmonary-vein isolation and posterior wall debulking [4]. The clinical outcome measured was AF recurrence one year post-ablation. Twenty-two patients with good-quality pre- and post-ablation MRI were included in this study. MRI quality was independently assessed by two experienced analysts, with inclusion requiring consensus on the absence of major artifacts and adequate contrast, especially in the right atrium.

2.2. Construction of Bi-atrial DTs

The bi-atrial DTs were constructed from pre- and post-ablation MRI scans. In short, automatic segmentation of the right and left atrium (LA) was done using a convolutional deep neural network [5], followed by manual quality control. Using personalized image intensity ratio, the

atrial wall was characterized as non-fibrotic, fibrotic (subdivided into interstitial and dense fibrosis), and exclusively in the post-ablation LA, also as ablation scar. Volumetric meshes, incorporating patient-specific atrial geometry and fibrosis/scar distribution, were generated. Then, atrial fibers, computed from diffusion tensor MRI data, were mapped onto the patient-specific meshes using Universal Atrial Coordinates [6]. Non-fibrotic and fibrotic cells were assigned EP parameters as described previously in detail [2]. We used a modified version of the Courtemanche model [7], and in fibrotic regions, we decreased IK1, ICaL, and INa conductance by 50%, 50%, and 40%, respectively. In contrast to previous studies, here we differentiate between two types of fibrosis – interstitial and dense fibrosis – representing different degrees of structural remodeling and differing only in their conduction velocities (where conduction through dense fibrosis was 50% slower than through interstitial fibrosis). Scar regions were modeled as non-conductive.

2.3. Assessment of the Arrhythmogenic Propensity of the Substrate in DTs

We assessed substrate arrhythmogenicity through EP simulations using openCARP [8] and followed our previously described sequential pacing protocol using 40 pacing sites [2] (Figure 1). For each DT, the substrate was deemed arrhythmogenic if at least one reentry (i.e., rotational activity sustained for at least three seconds) was observed upon cessation of pacing. For each patient, substrate arrhythmogenicity was first assessed in the pre-ablation DT. If the pre-ablation DT was arrhythmogenic, then substrate arrhythmogenicity was assessed in the corresponding post-ablation DT; otherwise, the DT pair was excluded from further analysis.

For each DT, we quantified the vulnerability – calculated as the ratio of pacing sites that induced a reentry to the total number of pacing sites used in the pacing protocol – as well as the potential reentry-sites (PRs) – representing the unique locations capable of sustaining reentries.

It is important to note that substrate arrhythmogenicity represents a measure of the substrate's likelihood of developing an arrhythmia, which may not necessarily represent the patient's current AF status (or lack thereof), as the manifestation of AF may be influenced by other factors such as ectopic triggers, parasympathetic and sympathetic inputs, etc.

3. Results and Discussion

3.1. Vulnerability to Reentry in DTs

Out of the twenty-two pre-ablation DTs, three had no PRs following the pre-ablation inducibility test; of these, two belonged to the no-recurrence group. For the remaining nineteen DTs, the pre-ablation vulnerability to reentry was similar between the recurrence (14.2±10.2%) and no-recurrence groups (15.0±11.2%; p=0.880; Figure 2). How-

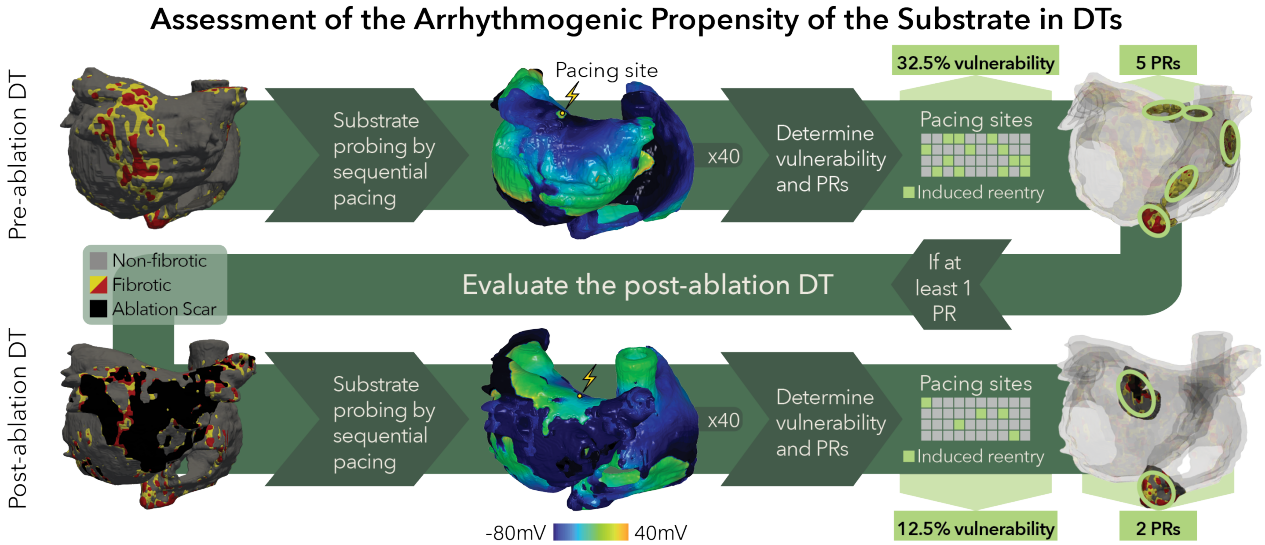

Figure 1. Protocol for assessing the arrhythmogenic propensity in DTs. First, the pre-ablation DTs were probed by sequential pacing from 40 different sites. If at least one reentry was induced in the pre-ablation DT, the corresponding post-ablation DT was evaluated using the same pacing protocol. The arrhythmogenic propensity of each DT was quantified by two metrics: vulnerability and number of PRs. In this example, the pre-ablation DT had 13/40 pacing sites that induced reentry (vulnerability=32.5%) in 5 different PRs, and the post-ablation DT had 5/40 pacing sites that induced reentry (vulnerability=12.5%) in 2 different PRs.

ever, following the procedure, the DTs of patients whose AF recurred post-ablation (R-DTs) exhibited an increase in vulnerability (Δ vulnerability=9.0±17.2%), while the DTs of patients whose AF did not recur (N-DTs) exhibited a decrease (Δ vulnerability=-8.3±8.4%; p=0.014). As a result, the post-ablation vulnerability was significantly higher in the recurrence group (23.2±17.5%) compared to the no-recurrence group (6.7±6.1%; p=0.015). These findings reveal that the ablation had opposite effects on substrate arrhythmogenicity in the two groups: it reduced the substrate's susceptibility to reentry in N-DTs, but increased it in R-DTs.

Our results indicate that high vulnerability observed at three months post-ablation is predictive of AF recurrence occurring within the first year following the procedure. This metric could serve as a tool for post-procedure risk stratification, helping to identify patients who may benefit from closer monitoring or adjunctive therapy after the ablation.

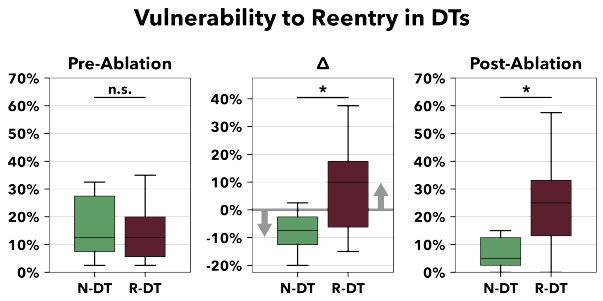

Figure 2. Vulnerability in N-DTs and R-DTs. Δ is the difference from pre- to post-ablation. Data are presented as median [IQR]. Statistical significance is indicated by an asterisk (p <0.05); $n.s.$ denotes non-significant differences.

3.2. Potential Reentry-Sites in DTs

In pre-ablation N-DTs, the average number of PRs was 3.9±2.8 (grey bars in Figure 3A), each induced by 1.5±1.0 pacing sites. In contrast, R-DTs exhibited a lower average of 2.3±1.5 PRs, each induced from 2.5±2.2 pacing sites. This suggests that despite fewer PRs in R-DTs pre-ablation, they were more easily inducible than in N-DTs, indicating that PRs in R-DTs were more arrhythmogenic.

From pre- to post-ablation, the average number of PRs in N-DTs decreased significantly (Δ PRs=-2.7±2.2), in contrast to R-DTs, where the average number of PRs decreased only slightly (Δ PRs=-0.2±1.8). This reduction in the number of PRs following the procedure was significantly different between the two groups (p=0.017), emphasizing their differential responses to ablation.

Post-ablation PRs were classified as residual (i.e., persisted from pre- to post-ablation) or emergent (i.e., seen only post-ablation). The number of residual PRs was low and similar in both groups: 3 out of 35 (9%) in N-DTs and 2 out of 23 (9%) in R-DTs, indicating that the ablation procedure eliminated most pre-ablation PRs in both groups. In contrast, there was a high incidence of emergent PRs, particularly in R-DTs. Most R-DTs had 2 or 3 emergent PRs (solid red bars in Figure 3A), while most N-DTs had only 1 (except for P9 with 2; solid blue bars in Figure 3A).

Our findings show that a reduction in the number of PRs correlates with a favorable outcome post-ablation (i.e., no-recurrence). Our analysis reveals that the ablation procedure was effective in eliminating most of the pre-existing PRs in both groups, but there was significant latent arrhythmogenicity in the recurrence group (i.e., emergent PRs), which could explain why AF recurred in these patients.

3.3. Scar-Anchored Reentries in Post-Ablation DTs

Approximately half of post-ablation PRs harbored reentries anchored around ablation scars. These scar-anchored reentries (ScAReentries) were nearly three times more prevalent in the recurrence group (11 ScAReentries in 7 R-DTs) than in the no-recurrence group (4 ScAReentries in 3 N-DTs; Figure 3B). Importantly, ScAReentries were inducible from more pacing sites (5.3±4.7 different sites) than reentries not anchored around scar (2.0±1.7; p=2·10^{-5}), contributing to higher vulnerability to reentry in post-ablation DTs.

From the post-ablation MRI scans, the absolute extent of ablation scar was greater in R-DTs (9.5±2.4 cm^3) than in N-DTs (6.7±2.0 cm^3; p=0.014). However, the relative extent of ablation-scar (i.e., the ratio of scar volume to LA atrial wall volume) was similar between the two groups (14.7±5.6% in N-DTs vs. 17.1±4.9% in R-DTs; p=0.079).

These findings demonstrate that ablation scars can create new arrhythmogenic substrates, as evidenced by ScAReentries. The heightened arrhythmogenic propensity in R-DTs is largely attributed to ScAReentries, which contributed to emergent PRs and a heightened vulnerability post-ablation. Our results suggest that the presence of ScAReentries may be a key factor in the clinical recurrence of AF after ablation. This underscores the clinical importance of recognizing the potential for ablation scars to create arrhythmogenic substrates and supports the need for further investigation into strategies that minimize these iatrogenic pro-arrhythmic effects.

4. Conclusion

In this study, we developed the first longitudinal bi-atrial DT framework to investigate the mechanisms underlying AF recurrence before and after catheter ablation. Our analysis reveals significant differences between the DTs of pa-

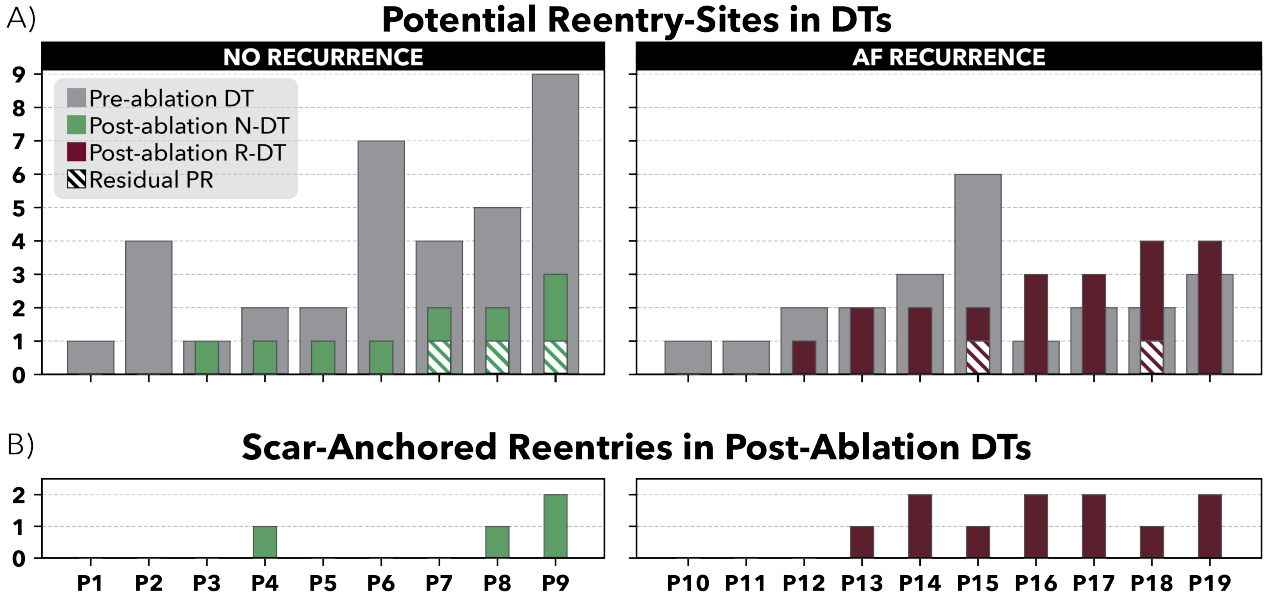

Figure 3. A) Number of pre- and post-ablation PRs for each DT-pair. B) Number of post-ablation PRs with scar-anchored reentries.

tients who did and who did not experience AF recurrence and suggests that the recurrence of AF may be facilitated by ablation lesions themselves. Our work demonstrates the value of computational models in elucidating the mechanisms underlying AF recurrence and highlights their potential for non-invasive, patient-specific risk stratification.

References

[1] Ganesan AN, Shipp NJ, Brooks AG, Kuklik P, Lau DH, Lim HS, Sullivan T, Roberts-Thomson KC, Sanders P. Long-term outcomes of catheter ablation of atrial fibrillation: A systematic review and meta-analysis. Journal of the American Heart Association 3 2013;2(2):e004549.

[2] Zahid S, Cochet H, Boyle PM, Schwarz EL, Whyte KN, Vigmond EJ, Dubois R, Hocini M, Haïssaguerre M, Jaïs P, Trayanova NA. Patient-derived models link re-entrant driver localization in atrial fibrillation to fibrosis spatial pattern. Cardiovascular research 6 2016;110:443–454. ISSN 1755-3245.

[3] Loewe A, Poremba E, Oesterlein T, Luik A, Schmitt C, Seemann G, Dössel O. Patient-specific identification of atrial flutter vulnerability-a computational approach to reveal latent reentry pathways. Frontiers in Physiology 1 2019; 10:425118. ISSN 1664042X.

[4] Segerson NM, Daccarett M, Badger TJ, Shabaan A, Akoum N, Fish EN, Rao S, Burgon NS, Adjei-Poku Y, Kholmovski E, Vijayakumar S, Dibella EV, MacLeod RS, Marrouche NF. Magnetic resonance imaging-confirmed ablative debulking of the left atrial posterior wall and septum for treatment of persistent atrial fibrillation: Rationale and initial experience. Journal of Cardiovascular Electrophysiology 2 2010;21:126–132. ISSN 1540-8167.

[5] Lefebvre AL, Yamamoto CAP, Shade JK, Bradley RP, Yu RA, Ali RL, Popescu DM, Prakosa A, Kholmovski EG, Trayanova NA. Lassnet: A four steps deep neural network for left atrial segmentation and scar quantification. Left atrial and scar quantification and segmentation first challenge LAScarQS 2022 held in conjunction with MICCAI 2022 Singapore September 18 2022 proceedings 2023;13586:1–15. ISSN 16113349.

[6] Roney CH, Pashaei A, Meo M, Dubois R, Boyle PM, Trayanova NA, Cochet H, Niederer SA, Vigmond EJ. Universal atrial coordinates applied to visualisation, registration and construction of patient specific meshes. Medical Image Analysis 7 2019;55:65–75. ISSN 1361-8415.

[7] Courtemanche M, Ramirez RJ, Nattel S. Ionic mechanisms underlying human atrial action potential properties: Insights from a mathematical model. American Journal of Physiology Heart and Circulatory Physiology 1998;275. ISSN 03636135.

[8] Plank G, Loewe A, Neic A, Augustin C, Huang YL, Gsell MAF, Karabelas E, Nothstein M, Prassl AJ, Sánchez J, Seemann G, Vigmond EJ. The opencarp simulation environment for cardiac electrophysiology. Computer methods and programs in biomedicine 7 2021;208. ISSN 1872-7565.

Address for correspondence:

Carolyna Yamamoto Alves Pinto
3400 N. Charles St., Hackerman Hall 216, Baltimore, MD 21218
cyamamo2@jhu.edu